



Waste Mass Movements Analysis of Dash-Kamel area by using the Stereographic Projection (Marzanabad-Chalus freeway)

Saeid Hakimi Asiabar*

Department of Geology, Islamic Azad University- Lahijan branch, Lahijan, Iran

ARTICLE INFORMATION

Received 02 April 2018

Revised 08 July 2018

Accepted 23 September 2018

KEYWORDS

Mass wasting; RMR rating; Chalus freeway; Stereographic Projection; Iran; Chalus freeway.

ABSTRACT

A mass wasting movement occurred along Chalus- Marzanabad freeway in March 2014 in Iran on which the most parts of the moved masses include soils with rock fragments. Province under construction freeway No. 3 is the main route from the capital city of Tehran to the Chalus city. The study area is located at the mileages between 5K and 6K along the freeway. Slope failures which triggered by earthquake activities and heavy rainfalls occur frequently. This paper is based on theoretical aspects and structural geology data for evaluation of the potential slope sliding behavior. The methodology is based on preparing topographic and geologic maps, measuring of layering and joints, preparing structural cross sections and rock mass rating of rock masses. According to RMR rating, Cohesion factor and friction angle of rock masses have been determined and used for analysis of mass wasting movements. This study showed an irrelevant relationship between the slippage behavior of the slopes and the stratum materials in the area. In this area, Infiltration of water into the shear zone of faults, swelling of the marlstone layers and the formation of flow in the clay bed cover has been the main cause of mass movements.

1. Introduction

Slope failures along highways usually occur as a result of earthquakes or heavy rain-falls. Slope failures have become one of the main geological disasters in northern Iran due to natural disasters affecting the environment. Factors affecting slope stability can be divided into two main categories: internal latent items and external inducements. Latent factors include slope type, property, structure, etc. Inducements include typhoons, heavy rain-falls, earthquakes, human factors, etc. Internal factors are the most fundamental sources affecting slope stability, especially on rocky slopes. Inducements, on the other hand, are direct causes of slope instabilities. Relatively, wedge sliding occurs more frequently on mountain highway slopes because of the landscape undulation, the failure mechanism of which consists of two or more sets of discontinuous planes with well-developed joints. Wedge failures may occur when the angle between two discontinuous planes is smaller than the dip angle and larger than

the friction angle. The regional rock stratum has a strong effect on the stability analysis of slopes, particularly regarding the potential risks of dip-slopes. Plane altitude of stratum is usually expressed in a strike and dip angle. Usually, mountain highway instabilities occur on rocky slopes. Site probe investigation should be conducted in the analysis. The instability study of slopes can be carried out by applying the data of discontinuous planes' stratum and gradient. Also, stereographic projection or slope stability equation may be used to assess the instability of highway slopes (Azarafza et al., 2013; 2014). Bishop (1995) first applied the Equal-Angle Projection Method in slope sliding stability analysis. Phillips (1972) used the Stereographic Projection Method for estimating the effects of geologic structures in slope sliding stability. Goodman (1976) utilized the Stereographic Projection Method in the joints investigation of rock's discontinuous planes. Hoek and Bray (1981) nominated a complete method to analyze slope wedges. Warburton (1981) analyzed the geometrical instability of polyhedron rocks by using vectors. Goodman and Shi (1985) introduced the Block Theory. By segmenting spatial

* Corresponding author.

E-mail address: saeid.h.asiabar@gmail.com
Assistant Professor, Academic Staff.

geometries, all of the geometries related to spatial volume can be determined systematically. Also, the key block can be found by studying the stratum of failure planes. Goodman (1995) on the other hand, illustrated the evolving failure modes of any polyhedron by using stereographic projection. Yoon et al. (2002) described the instability modes of rocks on slopes of multiple free surfaces by using stereographic projection. Projecting the three-dimensional lines and planes on two-dimensional planes is a useful approach in the stability evaluation of rock slopes. In the analysis of regional rock slope stability, geometries and mechanism of failures can be observed in the site investigation, which is often constrained by height, weak plane, stratum, and length of the slope. However, before slope failures occur, it is necessary to decide how to judge the geometrical volumes which have potential risks, forecast the collapse of the slope, and evaluate the stability of moving direction based on limited information, all of which are main components in the task of disaster prevention. The study area is located in the northern part of central Alborz (Fig. 1). This range comprises some active faults (Moghimi et al., 2015; Berberian and Yeats, 2017; Babaei et al., 2017; Hakimi Asiabar and Bagheriyan, 2018). Many rock units are displaced because of fault movements and have faulted contact with each other. Field observations and engineering geology indicate that over the last decade several landslides have occurred around the highway route. The last mass wasting occurred in May 2014 in Dash Kamel area which located on the border of the 5th kilometer of the Chalus- Marzan Abad freeway. These gravity movements occurred after a few rainy weeks. The study of the surface of the earth indicates that the slides are from a height of 60 meters above the free surface of the road, and the displaced material is a mixture of soil and rock fragments. This movement can be started because of instability in rock basement or in its soil cover. In this paper, we have an investigation on the study of instability in the rock basement with respect to the orientation of layering and joint sets. The purpose of this study is to investigate the probability of occurrence of motion factors in the basement rocks, in order to ensure the stability of the bedding, in addition to the stability of the soil and void, if necessary.

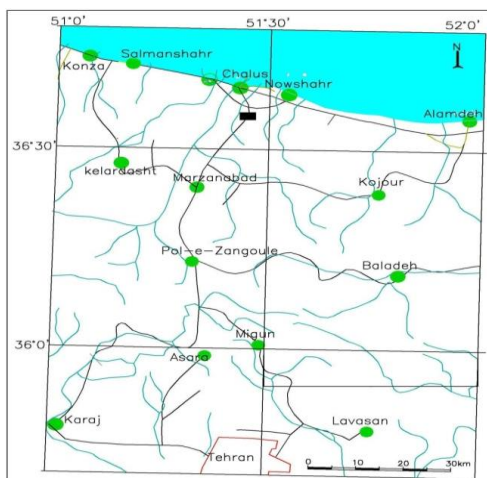


Figure 1. Location of the studied area

2. Material and Methods

According to the prepared geologic map and its structural cross section which prepared parallel to the freeway route, the mass wasting area divided into five blocks and these blocks separated from each other by faults with small displacement. On each block altitude of layering and joints is different from other blocks. The rock mass rating of each block held on the basis of Joint situations. In order to study the geological status of the studied area, a topographic and geological map of the landslide range was prepared at a scale of 1:1000. After plotting the altitude of the layers and joint sets, the longitudinal and transverse geological sections of the mass wasting area prepared.

The unstable area of the landslide classified into several blocks based on the deformation style and structural deformations of the rock units. In each of these blocks, the RMR classification of rock mass (Bieniawski, 1989) held on the basis of the condition of joint sets. The internal friction angle, rock adhesion coefficient, determined on the basis of rock mass classification. The probability of occurrence of gravitational movements in the basement of each block determined using the combination of geological data and RMR rating results and using Schmidt net.

2.1. Data Collection and Sampling

The excavations carried out for sampling at the project site included the drilling of three wells (TP-N2, TP-N3, TP-N1) with depths of 3 to 6 meters and two boreholes BH-A1, BH-A2 with a depth of 26 meters on the horizon of Soil and stone. The position of these boreholes is shown in Fig. 2. These digs have been carried out in order to obtain and control geological information, determining the thickness and physical and mechanical properties of topsoil cover, RQD, and other parameters of the rock masses of each block. According to the available information on the experiments performed on the cores, approximately the values of the resistance parameters of the soil and rock masses can be determined. Three samples sent for Brazilian testing and five samples for point load testing (Table 1 and 2). The results of the Brazilian test and the point load test are used for the classification of rock mass rating. The selection of rock mass parameters for designing cannot be limited to inadequate test results. Engineering judgments are usually applied by studying rocks and determining the classification of RMRs, GSI rankings, and rock Q ratings.

Table 1 Brazilian tensile test results

Sample No.	Tensile strength (MPa)	Depth (m)	Conditions
SN-1	37.6	42.18 - 49.18	Dry
SN-3	5.4	7.18 - 8.18	Dry
SN-4	59.2	88.19 - 95.19	Dry

Table 2 The results of the point load test

Sample No.	Point-load (MPa)	Depth (m)	Conditions
SN-1	27	42.18 - 49.18	Dry
SN-2	22	57.18 - 61.18	Dry
SN-3	27	7.18 - 8.18	Dry
SN-4	9	88.19 - 95.19	Dry
SN-5	31	50.25 - 53.25	Dry

2.2. Rock Mass Geomechanical Classification

In tunneling projects (Lu et al., 2010; Kulatilake and Jiang, 2013), the classification of the Q system usually perform (Barton et al., 1980), But this project is not related to the tunneling project, so the classification of the Q system is should not apply to these rock masses. The GSI classification system is based upon the supposition that the rock mass comprises plenty number of 'randomly' oriented discontinuities such that it seems like an isotropic mass (Hoek et al., 1998; Azarafza et al., 2017). In other words, in the GSI classification, the response of the rock mass is independent of the direction of the applied loads. Therefore, it is clear that the GSI system should not be applied to those rock masses which have a clearly defined dominant layering and structural orientation (Hoek et al., 2005). However, the Hoek–Brown criterion and the GSI chart can be used with prudence if the failure (Hoek and Diederichs, 2006) of such rock masses is not controlled by their anisotropy. It is also inappropriate to apply GSI values to excavated faces in strong hard rock with a few discontinuities spaced at distances of similar magnitude to the dimensions of the tunnel or slope under consideration. In such cases, the stability of the tunnel or slope will be controlled by the three-dimensional geometry of the intersecting discontinuities and the free faces created by the excavation. Obviously, the GSI classification does not assign to such cases.

3. Results and discussions

After preparing a geologic map and cross-sections which is presented in Fig. 2, the mass wasting area divided into five blocks. The deformation styles of these blocks are different from each other. Some of these blocks contain overturned folds, and some blocks only comprise of beds and faults. In each block, general characteristics of discontinuities described. Table 3 presents a summary of the field observations of the joint sets of aforementioned blocks. According to the characteristics of discontinuities, uniaxial strength, RQD and some descriptions of the surface of joint sets (Table 4), the RMR classification of rock masses carried out in all blocks.

3.1. Rock mass classification in block A

Block A is located in the southern margin of the Dash Kamel landslide and separated by a reverse fault of block B (Fig. 4a). In this block, the layers situation is N45E/75SE and includes marly limestone and marls. The thicknesses of marly limestones are less than 12 centimeters and the thickness of the marlstones are less than 5 centimeters. Block A in the RMR rating (Bieniawski, 1989) is considered a poor rock (Class IV).

3.2. Rock mass classification in block B

This block includes marly limestone and marls. The thicknesses of beds are less than 20 centimeters. This block truncated by a reverse fault with NW-SE trend. The dip of this fault is 75 to E. The width of the shear zone of this reverse fault is about 4-2 meters. In the central part of the shear zone of this fault, the grain size of particles is less than 1 mm which caused by the reverse motion of the fault. Most of the joint sets of block B have are less than 3 meters long, but about 25 percent of these joints have a length of 3-10 meters. Block B comprises recumbent fold

(Fig. 4b). The plunge of the fold axis of this fold is about 20° to the southwest. The lack of joint fillings and the presence of clay in block B are evident. Block B in the RMR rating (Bieniawski, 1989) is considered a very poor rock (Class V).

3.3. Rock mass classification in block C

In block C, the layers situation is N74E/65SE and comprises of marly limestone. The thicknesses of marly limestones are less than 10 centimeters and the thickness of the marlstones are less than 5 centimeters. The dip direction of the bedding surfaces in block C is not compatible with the slope direction of the topography and landslide. Block C is located in the central part of the Dash Kamel landslide and separated by two reverse faults of block B and D. There reverse fault between block B and block C and has a dip to the northwest. The situation of the fault between block C and block D is N90E/60S. There are some lineaments in the central part of the block C with W-E direction. Block C in the RMR rating (Bieniawski, 1989) system is considered a very poor rock (Class V).

3.4. Rock mass classification in block D

Block D comprises a recumbent fold (Fig. 4c) with a vengeance to the south. The plunge of the fold axis of this fold is about 10° to the southwest. This block includes marly limestone and marls. The situations of most of the layers in block D are N45E/75SE. The thicknesses of beds are less than 15 centimeters. Most of the joint sets of block D have are less than 3 meters long. The Dip direction of bedding in block D is not compatible with topographic slope direction. Rock masses of Block D in the RMR rating (Bieniawski, 1989) are considered as a poor rock (Class IV).

3.5. Rock mass classification in block E

Block E is located in the northern margin of the Dash Kamel landslide (Figs. 2 and 3) and separated by a reverse fault of block D (Fig. 4d). Block E comprises a recumbent fold with a vengeance to the south. This block includes marly limestone and some intercalations of very thin marl beds (less than 5 cm). The thickness of limestone beds in block E is about 10-18 centimeters. The Dip direction of bedding in block E is not compatible with topographic slope direction and transitional landslide cannot occur in Block E. The rock mass of the block E in the RMR rating system is considered as a poor rock (Class IV). In the rock mass rating classification Tables (Bieniawski, 1989), values for the internal friction angle and cohesion of rock mass of each block are presented in Table 4. In the research on structural geology, stereographic projection is applied to indicate the rock's structural plane on projection drawings to confirm the relationship between their angles. Stereonet is mainly used to project the three-dimensional geological structure on two-dimensional planes.

By understanding the distribution of the weak planes, analyses of rock stratum and relative angles can carry out for rock stability analysis; they are most used in stability analysis on rock slopes and tunnels. This method can be applied to underground excavation, rock classification, and rock slope construction and is most useful in regard to rock slope construction (Grenon & Hadjigeorgiou 2008).

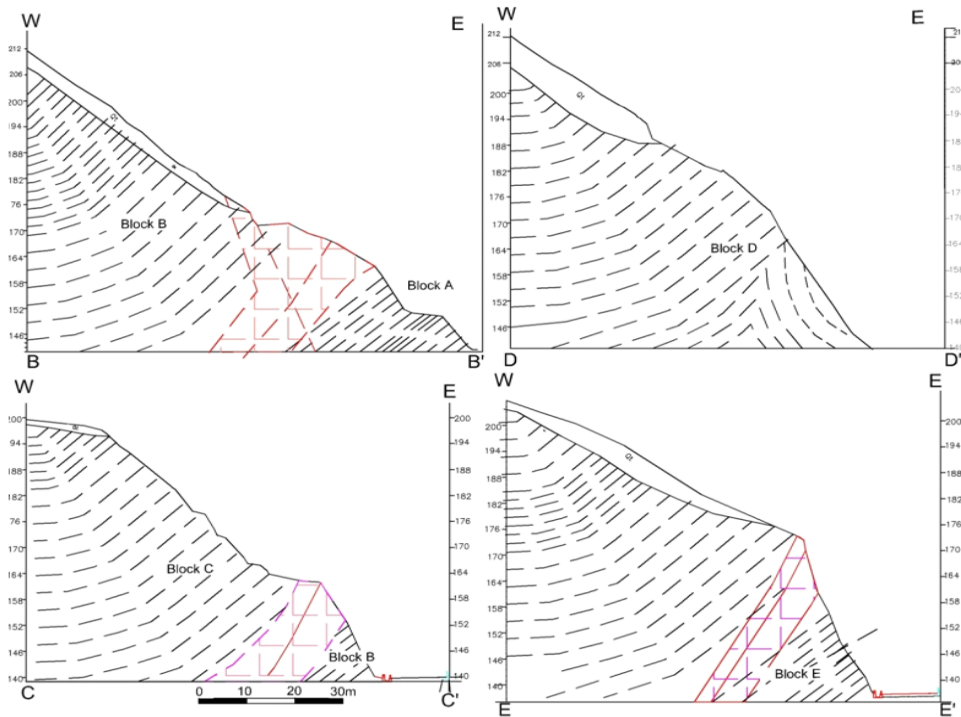
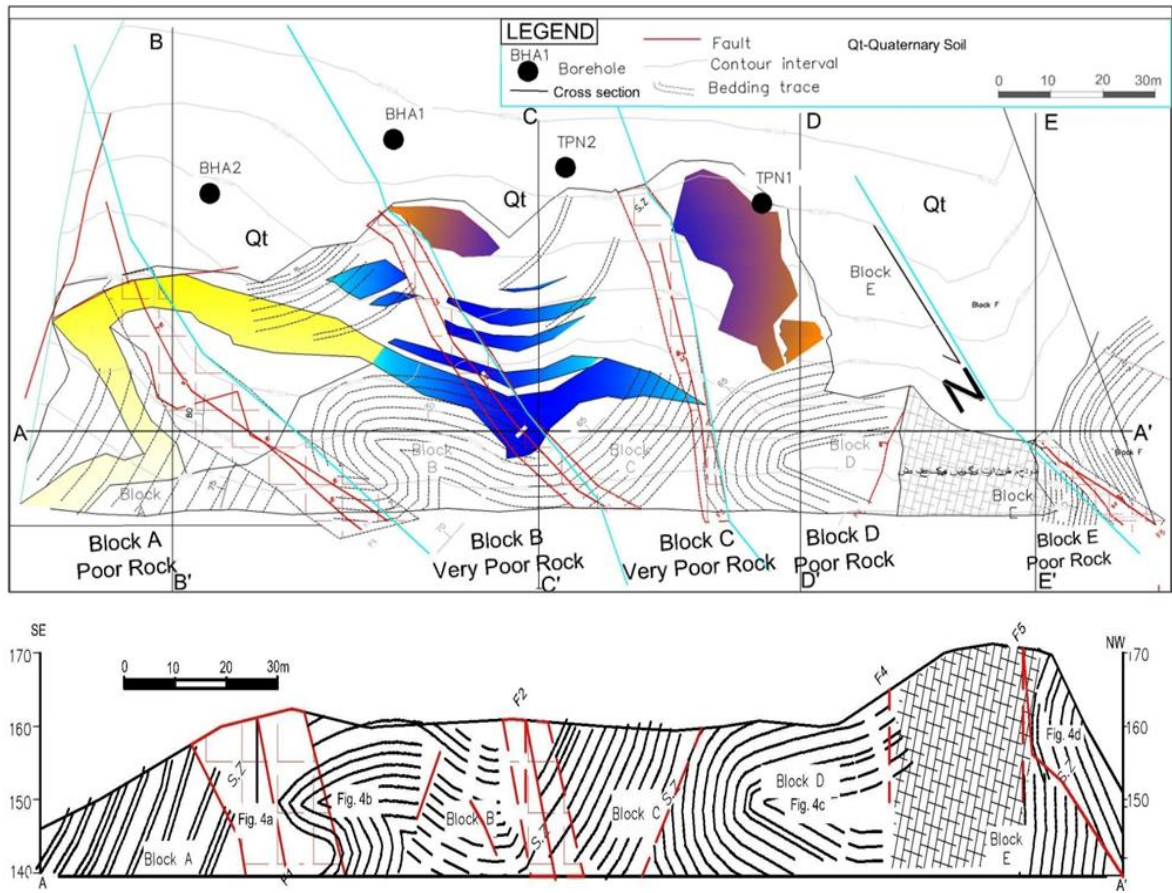


Figure 3. Perpendicular Cross sections of the road

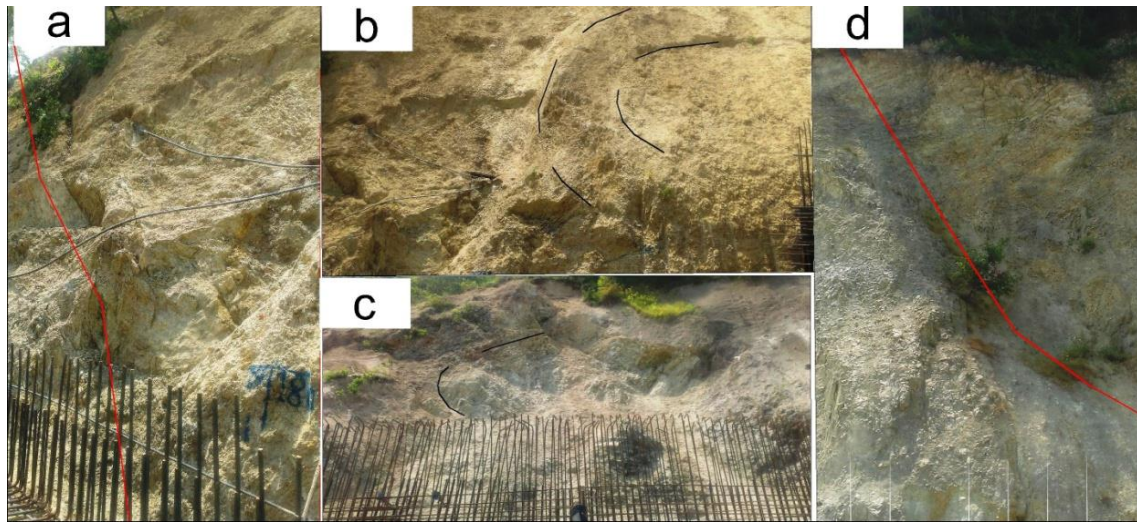


Figure 4. Perpendicular Cross sections of the road

Table 3 Summary of field observations on the properties of joints of different blocks

Parameter	Blocks				
	Block A	Block B	Block C	Block D	Block E
Opening	0.1-1 mm	1-5 mm	1-5 mm	0.1-1 mm	1-5 mm
Conditions of discontinuities	Slightly rough	slightly rough	slightly rough	Slightly rough	slightly rough
Filling	soft filling	soft filling	soft filling	hard filling	soft filling
Weathering	Moderately weathered	moderately weathered	moderately weathered	moderately weathered	slightly weathered
Ground water	dry	wet	Wet	dry	dry
Length of Discontinuities	10-20 m	more than 20 m	more than 20 m	10-20 m	10-20 m

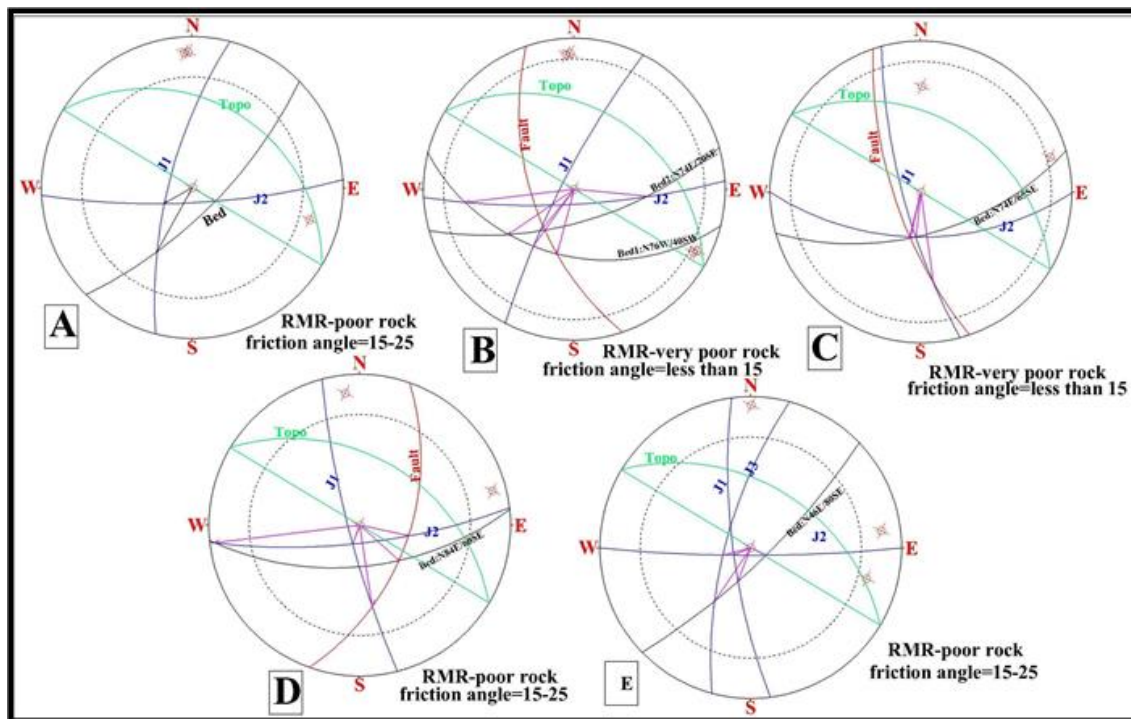


Figure 5. Equal area projection of the layers (black planes), faults (red planes) the joint sets (J1, J2, J3), and the topography (green surface), the friction angle (dotted circle) and the intersection lines of discontinuities.

Table 4 RMR based rock engineering classification

Blocks	RMR rating	Cohesion (MPa)	Friction (deg.)
A	IV	100 - 200	15 - 25
B	V	<100	<15
C	V	<100	<15
D	IV	100 - 200	15 - 25
E	IV	100 - 200	15 - 25

Stereographic projection drawings simplify complicated and discontinuous three-dimensional space to two-dimensional planes. Although an accurate safety coefficient is not guaranteed, it is the most effective method for evaluating slope stability in the initial planning stage. On one hand, using this method can help to avoid construction on dangerous slopes. In this method, slope-related problems can be predicted and protective measures applied. Gokçeoglu et al. (2000) drew risk charts on slope failure in Turkey by using stereographic projection and kinematic analysis. Based on the forms of discontinuities and failures, in this research, we applied the Equal-Angle Projection Method to go on with the investigation of slope approaches, gradient, stratum trend, and dip angles.

This research also judged rock instability, studied its failure mechanism and direction. The combination of geological data usually held on the basis of the results of geomechanical classification of the rock mass, using the Equal angle projection, and by plotting bedding planes, Joint sets, and the internal friction angle of rocks. In this method, layers, joint sets and the internal friction angle of the rock mass of each block are depicted in the stereogram. These datasets can be explored and analyzed in the stereographic projection. Figure 4 shows the recommended plan for merging data in Equal-area projection which are defined as follows:

- The trend and plunge of the line of intersection of planes (such as Joint sets J1 and J2) can be determined on the stereographic projection. The intersection line of joint sets and bedding are represented by points where the two great circles of the planes intersect, and the line orientation is defined by its trend and its plunge,
- The internal friction angle plotted in the diagram with a dotted line circle,
- The inclination of the slope face measured from a topographic map and plotted in the diagrams.

3.6. Stereographic Analysis of Geological and Geotechnical Data in Block A

Block A is a domain of an asymmetric fold, and its bedding plane is not compatible with the direction of the topographic slope (Fig. 3). Two sets of joints and bedding are presented in this block (Fig. 5). The line of joint sets intersection is about 72° to the southwest, and the intersection line of bedding plane and joint set 1 (J1) and joint set 2 (J2), is about 45° to the southwest and 70° to southeast respectively. These intersection lines are inconsistent with the direction of the topographic slope face and cannot create sliding in rock mass of block A.

3.7. Stereographic Analysis of Geological and Geotechnical Data in Block B

Block B is a recumbent anticline with bedding situations N74E/70SE, N76W/40SW. The bedding planes of this fold are not compatible with the direction of the topographic slope (Fig. 3). Two sets of joints, a fault plane, and bedding planes are presented in this block. According to the Equal-area projection of block B (Fig. 5B):

- The joint sets intersection (Fig. 5B) is about 51° to the southwest,
- The intersection line of fault plane and joint sets are about 50°-55° to south and southwest,
- The intersection line of bedding planes, fault, and joint sets have several directions (and dips between 28°- 50°) but don't have the same direction with topography.,

The intersection lines of planes in block B are inconsistent with the direction of the topographic slope face and cannot create sliding and wedge failure in rock mass of block B. Therefore the failure factor in rock mass in block B is judged as stable.

3.8. Stereographic Analysis of Geological and Geotechnical Data in Block C

In block C, the layers situation is N74E/65SE and comprises of marly limestone. The bedding plane of this block is not compatible with the direction of the topographic slope. Two sets of joints and a fault plane with bedding planes are presented in this block (Fig. 5c). According to the Equal-area projection of block B (Fig. 5c), the azimuth of intersection lines of planes in block C are 170°-220° and are inconsistent with the direction of the topographic slope and cannot create sliding wedge failure and toppling in rock mass of block C. Therefore the failure situation in rock mass of block C is judged as stable.

3.9. Stereographic Analysis of Geological and Geotechnical Data in Block D

In block D, the layers situation is N84E/60SE and comprises of marly limestone. The bedding plane and fault plane of this block are not compatible with the direction of the topographic slope. Two sets of joints and a fault plane with bedding planes are presented in this block (Fig. 5d). According to the Equal-area projection of block D (Fig. 5d), the azimuth of intersection lines of planes in block D is 100°-230° and are inconsistent with the direction of the topographic slope and cannot create sliding and wedge failure in rock mass of block D but the lines of intersections between joint set 1 and joint set 2 (J1 and J2) has 85/230 situation and nearly can create toppling of falling of rock fragments in this block but it can be controlled by creating a retaining wall.

3.10. Stereographic Analysis of Geological and Geotechnical Data in Block E

In block E, the layers situation is N46E/80SE. The bedding plane of this block is not compatible with the direction of the topographic slope. Three sets of joints are presented in this block (Fig. 5E). According to the Equal-area projection of block E (Fig. 5E), the azimuth of intersection lines of planes in block E are 100°-230° and are inconsistent with the direction of the topographic slope and cannot create sliding and toppling in rock

mass of block E. Therefore the failure situation of block E is judged as stable.

4. Conclusion

This study shows that different kinds of discontinuities (joints, faults and shear zones) cutting by the trench due to a man-made activity which affects the stability of the slope and creates the mass movement in the study area.

- Rock mass rating (RMR) and graphical analysis of the discontinuities and joint sets indicate the study area is not a landslide-prone zone and therefore the mass wasting occurred because of instability in soil cover. This study will be helpful in assisting the ongoing civil work in the study area.
- In this area, water penetration in the brecciated zone of faults, swelling of the marlstone layers, and the absorption of water in the topsoil cover was the main reason of mass movements.
- In block D and block A, there is a weak possibility of toppling and falling which can be controlled by the setting up of a retaining wall. The presence of water changed the spatial status of discontinuities in these blocks and made them close to the critical situation, therefore drainage of the upstream area of the Dash Kamel landslide will increase the stability of this area.

Acknowledgements

The authors wish to thank the Mr. Gholami and Dr. Torabi, who are the chief executives of the Dash Kamel landslide project in the “Khak Va Sang” company for giving the soil tests lab and preparing experiments studies.

REFERENCES

- Azarafza M., Akgün H., Asghari-Kaljahi E. (2017). Assessment of rock slope stability by slope mass rating (SMR): A case study for the gas flare site in Assalouyeh, South of Iran. *Geomechanics and Engineering*, 13(4): 571-584.
- Azarafza M., Asghari-Kaljahi E., Moshrefy-Far M.R. (2014). Numerical Modeling and Stability Analysis of Shallow Foundations Located Near Slopes (Case Study: Phase 8 Gas Flare Foundations of South Pars Gas Complex). *Journal of Geotechnical Geology*, 10(2): 92-99.
- Azarafza M., Yarahmadi-Bafghi A.R., Asghari-Kaljahi E., Bahmannia G.R., Moshrefy-Far M.R. (2013). Stability analysis of jointed rock slopes using the key block method (case study: gas flare site in 6, 7 and 8 phases of South Pars Gas Complex). *Journal of Geotechnical Geology*, 9(3): 169-185.
- Babaei S., Dehbozorgi M., Hakimi Asiabar S. (2017). Assessment of active tectonics by using morphometric indices in Central Alborz. *Quarterly Quantitative Geomorphological researches*, 6(1): 40-56.
- Barton N., Løset F., Lien, R., Lunde J. (1980). Application Of Q-System In Design Decisions Concerning Dimensions And Appropriate Support For Underground Installations. In: *Proceedings of the ISRM International Symposium - Rockstore*, Stockholm, Sweden, June 1980.
- Berberian M., Yeats R.S. (2017). *Tehran: An earthquake time bomb*. In GSA Special Papers: Tectonic Evolution, Collision, and Seismicity of Southwest Asia: In Honor of Manuel Berberian's Forty-Five Years of Research, DOI: 10.1130/2016.2525(04).
- Bieniawski Z.T. (1989). *Engineering rock mass classifications*. Wiley-Interscience, 272 p.
- Bishop A.W. (1995). The use of the slip circle in the stability analysis of slopes. *Geotechnique*, 5: 7-17.
- Gokçeoglu C. Sonmez H., Ercanoglu M. (2000). Discontinuity controlled probabilistic slope failure risk maps of the Altındag (settlement) region in Turkey. *Engineering Geology*, 55: 277-296.
- Goodman R.E. (1976). *Methods of Geological Engineering in Discontinuous Rocks*. West Group press, 484 p.
- Goodman R.E. (1995). Block theory and its application. *Geotechnique*, 45(3): 383-423.
- Goodman R.E. Shi G.H. (1985). *Block Theory and Its Application to Rock Engineering*. Prentice-Hall International, 338 p.
- Grenon M., Hadjigeorgiou J. (2008). A design methodology for rock slopes susceptible to wedge failure using fracture system modeling. *Engineering Geology*, 96: 78-93.
- Hakimi Asiabar S., Bagheriyan S. (2018). Exhumation of the Deylaman fault trend and its effects on the deformation style of the western Alborz belt in Iran. *International Journal of Earth Sciences*, 107(2): 539-551.
- Hoek E., Bray J.W. (1981). *Rock Slope Engineering (3rd Edition)*. CRC Press, 364 p.
- Hoek E., Diederichs M.S. (2006). Empirical estimation of rock mass modulus. *International Journal of Rock Mechanics and Mining Sciences*, 43: 203-215.
- Hoek E., Marinos P. Benissi M. (1998). Applicability of the geological strength index (GSI) classification for very weak and sheared rock masses. The case of the Athens Schist Formation. *Bulletin of Engineering Geology and the Environment*, 57(2): 151-160.
- Hoek E., Marinos P. Marinos V. (2005). Characterization and engineering properties of tectonically undisturbed but lithologically varied sedimentary rock masses. *International Journal of Rock Mechanics and Mining Sciences*, 42(2): 277-285.
- Kulatilake P.H.S.W., Jiang F. 2013. Investigation of stability of a tunnel in a deep coal mine in China. *International Journal of Mining Science and Technology*, 23: 463-624.
- Lu M., Grøv E., Holmøy K.H., Trinh N.Q., Larsen T.E. (2010). Tunnel Stability And In-situ Rock Stress. In: *Proceedings of the International Symposium on In-Situ Rock Stress*, Beijing, China, August 2010.
- Moghimi M., Arian M. Sorbi A. (2015). Fault Movement Potential of Marzanabad Area. North Alborz, Iran, *Open Journal of Geology*, 5: 126-135.
- Phillips F.C. (1971). *The use of stereographic projection in structural geology (3rd Edition)*. Edward Arnold, 90 p.
- Warburton P.M. (1981). Vector Stability Analysis of an Arbitrary Polyhedral Rock Block with any Number of Free Faces. *International Journal of Rock Mechanics and Mining Sciences & Geomechanics Abstracts*, 18: 415-427.
- Yoon W.S., Jeong U.J., Kim J.H. (2002). Kinematic analysis for sliding Failure of Multi-faced rock slopes. *Engineering Geology*, 67: 51-61.